sATP-binding cassette subfamily G member 2 enhances the multidrug resistance properties of human nasal natural killer/T cell lymphoma side population cells

SHAOXUAN WU[1-3*], XUDONG ZHANG[1,3*], MENG DONG[1,3],
ZHENZHEN YANG[1,2], MINGZHI ZHANG[1,3] and QINGJIANG CHEN[1,3]

[1]Department of Oncology, The First Affiliated Hospital of Zhengzhou University;
[2]Academy of Medical Science, Zhengzhou University, Zhengzhou, Henan 450052;
[3]Lymphoma Diagnosis and Treatment Center of Henan Province, Zhengzhou, Henan 450000, P.R. China

Abstract. Extranodal natural killer (NK)/T cell lymphoma, nasal type (ENKL) is a rare type of non-Hodgkin's lymphoma that is associated with limited effective treatment options and unfavorable survival rate, which is partly the result of multidrug resistance (MDR). The presence of side population (SP) cells-SNK-6/ADM-SP (SSP) cells has been previously used to explore mechanisms of drug resistance. ATP-binding cassette subfamily G member 2 (*ABCG2*) is a gene involved in MDR and is closely associated with SPs. However, the function of ABCG2 in SSP cells is unclear. The present study verified the high expression of ABCG2 in SSP cells. The IC_{50} values of doxorubicin, cytarabine, cisplatin, gemcitabine and l-asparaginase were tested to evaluate drug sensitivity in SSP cells with different levels of ABCG2 expression. *ABCG2* was identified as a gene promoting in MDR. ABCG2 upregulated cell proliferation, increased clonogenicity, increased invasive ability and decreased apoptosis, *in vivo* and *in vitro*, when cells were treated with gemcitabine. To conclude, ABCG2 enhanced MDR and increased the typical biological characteristics associated with cancer cells in SP cells. With further investigation of the *ABCG2* gene could have the potential to reverse MDR in ENKL.

Correspondence to: Dr Qingjiang Chen or Dr Mingzhi Zhang, Department of Oncology, The First Affiliated Hospital of Zhengzhou University, 1 Jianshe Road, Zhengzhou, Henan 450052, P.R. China
E-mail: qingjiang_c@126.com
E-mail: mingzhi_zhang1@163.com

*Contributed equally

Introduction

Extranodal natural killer (NK)/T cell lymphoma (ENKL) is an aggressive malignant lymphoma that occurs frequently in Asian countries, where it accounts for >10% of non-Hodgkin lymphoma (NHL), but rarely in Western countries, where it contributes to <1% of NHL cases (1-3). Localized ENKL that are treated with the incorporation of radiation and chemotherapy have good clinical outcomes with a 5-year progression-free survival rate of 61% and an overall survival rate of 72% (4). Likewise, survival has improved in disseminated disease. However, a significant percentage of metastatic ENKL will recur or exhibit refractory disease despite the initial benefit from multi-agent chemotherapy regiments (4,5). The optimal treatment for these relapsed disease is unknown (6,7) and the underlying causes for the development of ENKL are multifactorial and complex (8).

Numerous tumors are comprised of a hierarchical heterogeneous structure reminiscent of side population (SP) system, with more primitive and more therapy-resistanT cell types (9,10). Numerous studies have demonstrated that multi-drug resistance (MDR) leads to tumor recurrence, which is hypothesized to be caused by SP cells (11,12). SP cells have been identified based on their ability to export Hoechst 33342 dye via various members of the ATP-binding cassette (ABC) membrane transporter family of proteins, which are highly expressed in SP cells (9,10,12-14).

These hypotheses led to the identification of a novel method to investigate ENKL cell lines using SP cells. We previously demonstrated that SNK-6/ADM-SP (SSP) cells that presented the mature NK cell-derived phenotype and indolenT cellulated features showed higher MDR compared with SNK-6 cells (15). A noteworthy property of SSP cells is their high expression of ABC efflux transporters, especially ATP-binding cassette subfamily G member 2 (ABCG2). Previous studies have reported that ABCG2 can decrease intracellular anticancer drug concentrations, which can contribute to chemoresistance in various types of tumors (16-18). However, the function of ABCG2 in SSP cells and ENKL progression remains unclear. Therefore, SSP cells were used to investigate the role of ABCG2 and identify a novel method to treat drug-resistant ENKL cells.

The present study aimed to analyze the relationship among ABCG2, traditional chemotherapy drugs and biological characteristics of ENKL SSP cells *in vitro* and *in vivo*. In addition to broadening our understanding of SP cells, the present study may have identified a novel antitumor mechanism that could be of use to reestablish the sensitivity of SSP cells to chemotherapy to yield clinical benefit.

Materials and methods

Cell culture. SNK-6 cells were established from primary lesions with nasal NK-cell lymphoma [CD3ε+, CD20-, CD56+, CD3 (Leu4)-, EBV-encoded small RNA+ (EBER+)] and were kindly provided by Dr Norio Shimizu of Chiba University (Chiba, Japan) (19). Their team originally established SNK-6 cell line from primary lesions of a Japanese patient with nasal T/NK-cell lymphoma (19). SNK-6 cells were CD3- CD4- CD8- CD16- CD19- CD21-CD25+ CD56+ CD57+ HLA- DR+, and exhibited the NK-cell phenotype (15,20). SSP cells were provided by Dr Xudong Zhang of Department of Oncology, The First Affiliated Hospital of Zhengzhou University, China. Their team sorted SSP cells via a Hoechst 33342 assay from SNK-6 cells and verified the NK-cell phenotype (15). SNK-6 and SSP cells were cultured in RPMI-1640 medium (Gibco; Thermo Fisher Scientific, Inc.) supplemented with 5% UltraGRO™ Advanced cell culture supplement (AventaCell BioMedical Corp, Ltd.), 100 U/ml penicillin, 100 μg/ml strep-tomycin, 2 mM L-glutamine, 0.05 mM β-mercaptoethanol, 0.02% sodium bicarbonate and 1,000 IU/ml interleukin (IL)-2.

Flow cytometric analysis. To evaluate lymphocytic surface antigens, the expression levels of lymphocytic molecular markers (CD3-, CD5-, CD8-, CD56+, CD16-, Granzyme B+ and Perforin+) of SSP cells were confirmed (15,19,20). Unstained SSP cells were used for the negative control. In total, $1x10^6/100$ μl SSP cells were resuspended in PBS (HyClone; Cyvita; cat. no. SH30256.01) were incubated with anti-CD3 (5 μl ready to use; PerCP Mouse Anti-Human; cat. no. 552851), anti-CD8 (5 μl ready to use; FITC Mouse Anti-Human, cat. no. 561948) and anti-CD56 (5 μl ready to use; PE-Cy™ 7 Mouse Anti-Human; cat. no. 557747) (all BD Pharmingen™; BD Biosciences) at room temperature (RT) for 15 min. Then intrasure reagent A and B (BD IntraSure™ kit; cat. no. 641776) were used to fix and permeabilize cells according to the manu-facturer's instructions. Then Granzyme B (5 μl ready to use; BD Pharmingen™; BD Biosciences; PE Mouse Anti-Human, cat. no. 561142) and Perforin (5 μl ready to use, BD Horizon™; BD Biosciences BV421 Mouse Anti-Human, cat. no. 563393) were incubated for 15 min at RT. Another tube of the same SSP cells were incubated with anti-CD5 (5 μl ready to use; PE Mouse Anti-Human; cat. no. 555353) and anti-CD16 (5 μl ready to use; FITC Mouse Anti-Human; cat. no. 561308) (both BD Pharmingen™; BD Biosciences) for 15 min at RT. All the cells were examined using a flow cytometer (FACSCantoII) and FACSDiva software version 6.1.2 (both BD Biosciences).

Lentiviral transduction and selection of stable cell lines. *ABCG2* cDNA and shRNA targets (Shanghai GeneChem Co., Ltd.) were designed according to the *ABCG2* gene sequence (gene number: AY017168). In total, 7.5 μg purified plasmids pCDH-CMV-MCS-EF1-copGFP-vector, pCDH-CMV-MCS-EF1-copGFP-ABCG2, pCDH-CMV-MCS-EF1-copGFP-sh-control, pCDH-CMV-MCS-EF1-copGFP-ABCG2-SH1 (target1,1462; 5'-GCAGGATAAGCCACTCATA-3'), pCDH-CMV-MCS-EF1-copGFP-ABCG2-SH2 (target2, 2078; 5'-GCAGGTCAGAGTTGGTTT-3'), pCDH-CMV-MCS-EF1-copGFP-ABCG2-SH3 (target3, 2208; 5'-GCATTCCACGATATGGATT-3') (all Shanghai GeneChem Co., Ltd.) were cotransfected with 6.4 μg packaging plasmid pCMV deltaR8.2 (Addgene, Inc.) and 1.1 μg envelope plasmid VSV-G (Addgene, Inc.) in 1,500 μl RPMI-1640 medium (Gibco; Thermo Fisher Scientific, Inc.) into HEK293T cells (American Type Culture Collection) using 30 μl Lipofectamine® 2000 (Invitrogen; Thermo Fisher Scientific, Inc.) according to the manufacturer's protocol at 37°C. The supernatant of HEK293T cells was discarded 8 h later and carefully added to 10 ml 1640 complete medium. After 72 h, the virus supernatant was collected, concentrated with Lenti-Concentin Virus Precipitation solu-tion (ExCell Bio, cat. no. EMB810A-1) and coinfected with SSP cells $(1x10^6/2$ ml) in the presence of 8 mg/ml polybrene (cat. no. sc-134220; Santa Cruz Biotechnology, Inc.). GFP was used to sort infected cells using a flow cytometer (FACS Aria III; BD Biosciences) and the results was analyzed by FACSDiva software version 6.1.2 (BD Biosciences) and showed that the purity of the transfected cells was >95%. In summary, six cell lines were successfully cultivated, including SSP-EV for lenti negative control, SSP-ABCG2 for *ABCG2* overexpression, SSP-sh-control for lenti-sh negative control and SSP-ABCG2-sh1-3 for *ABCG2*-knockdown.

Proliferation and IC_{50} assay. A total of $2x10^4$ cells/well seeded in 96-well plates were cultured in 90 μl RPMI-1640 medium supplemented as aforementioned (Gibco; Thermo Fisher Scientific, Inc.) at 37°C for 12 h and then treated with 10 μl doxo-rubicin, cytarabine, cisplatin, gemcitabine and L-asparaginase (all Sigma-Aldrich; Merck KGaA) separately in each well with a concentration gradient for 48 h. Cell Counting Kit (CCK)-8 solution (20 μl, 5 mg/ml; Dojindo Molecular Technologies, Inc.) was used to detect the activity of cells according to the manufacturer's instructions. The absorbance was measured at 450 nm using a Multiskan FC microplate reader (Thermo Fisher Scientific, Inc.). The inhibition rate (%) was calculated as follows: $(OD_{control}-OD_{treatment}/OD_{control})$ x100. Independent experiments were repeated at least three times.

EdU assay. EdU (5-ethynyl-2'-deoxyuridine) is a nucleoside analog to thymidine and incorporated into DNA during active DNA synthesis (21). Flow cytometry was performed to evaluate the proliferative ability of the SSP, SSP-EV, SSP-ABCG2 and SSP-ABCG2-SH cells using a Click-iT™ EdU Flow cytom-etry Assay kit (cat. no. C10634; Thermo Fisher Scientific, Inc.). Cells ($1x10^6$ cells/ml) were suspended in 100 μl PBS (HyClone; Cyvita; cat. no. SH30256.01) and incubated with EdU (10 μM) for 2 h at 37°C in the dark. After washing with PBS (HyClone; Cyvita; cat. no. SH30256.01), centrifuging (300 x g for 5 min at RT) and dislodging the pellet, the cells were treated with Click-iT™ fixative and permeabilization (cat. no. C10634; Thermo Fisher Scientific, Inc.) for 15 min at RT. Then the cells were labeled with 1xAlexa Fluor™ 647 picolyl azide (cat. no. C10634; Thermo Fisher Scientific, Inc.) in DMSO for

30 min at 37°C in the dark. Stained samples were analyzed using FACSCantoII (BD Biosciences) and FACSDiva software version 6.1.2 (BD Biosciences). The results were analyzed using FlowJo™ version 10 software (FlowJo LLC).

Immunocytochemistry. The SSP, SSP-EV, SSP-ABCG2 and SSP-ABCG2-SH cells were fixed with 4% paraformaldehyde (for 30 min at RT), following which the cell suspension was adhered to a slide with charged substrates using acetone (10 min, RT). After washing with PBS, the 0.5% Triton X-100 (10 min, RT) was added, and then cells were blocked with 3% BSA (Sigma-Aldrich; Merck KGaA) for 1 h at RT. Cells were then incubated with the ABCG2 antibody (1:200; cat. no. sc-58222; Santa Cruz Biotechnology, Inc.) at 4°C overnight, following this, the slide was incubated with the Goat anti-Mouse IgG (H+L) Cross-Adsorbed Secondary Antibody APC (1:100; cat. no. A-865; Invitrogen; Thermo Fisher Scientific, Inc.) and finally counterstained with DAPI (2 µg/ml; cat. no. 4084; Cell Signaling Technology, Inc.). Images were captured using a fluorescence microscope (400x magnification, DMI400B; Leica Microsystems GmbH).

Western blot analysis. Proteins of the SSP, SSP-EV, SSP-ABCG2 and SSP-ABCG2-SH cells were extracted using RIPA lysis buffer (Beyotime Institute of Biotechnology; cat. no. P0013B) containing protease inhibitor, phosphatase inhibitor and EDTA. After determining the protein concentration (BCA protein concentration determination kit; Beyotime Institute of Biotechnology; cat. no. P0012), 20 µg proteins were loaded per lane on a 10% gel, resolved using SDS-PAGE and then transferred to a PVDF membrane (Beyotime Institute of Biotechnology) by electroblotting. Then, the membrane was blocked with 1% BSA powder (Sigma-Aldrich; Merck KGaA) for 1 h at RT. The membrane was incubated overnight at 4°C with the following primary antibodies: ABCG2 (1:500; cat. no. 42078; Cell Signaling Technology), Bax (1:1,000; cat. no. 5023; Cell Signaling Technology), BCL2 (1:1,000; cat. no. 15071; Cell Signaling Technology), Bad (1:500; cat. no. 10435-1-AP; ProteinTech Group, Inc.), Myc proto-oncogene protein (c-Myc) (1:500; cat. no. 10828-1-AP; ProteinTech Group, Inc.) and GAPDH (1:3,000; cat. no. 60004-1-Ig; ProteinTech Group, Inc.). Secondary antibodies, goat anti-rabbit IgG (1:8,000; cat. no. 10285-1-AP; Cell Signaling Technology, Inc.) and goat anti-mouse IgG (1:8,000; cat. no. SA00001-1; Cell Signaling Technology, Inc.) were then incubated with the membrane for 1 h at RT. Signals were detected using an ECL detection reagent (Santa Cruz Biotechnology, Inc.). Images of the band images were captured and quantified using the ChemiDoc™ XRS+ system (Bio-Rad Laboratories). ImageJ version 1.52a software (National Institutes of Health) was used to analyze the greyscale values of the protein bands.

RNA isolation and reverse transcription-quantitative (RT-q)PCR. Total RNA were extracted from of SSP, SSP-EV, SSP-ABCG2, SSP-sh-control, SSP-ABCG-sh1, SSP-ABCG2-sh2 and SSP-ABCG2-sh3 cells with TRIzol® reagent (cat. no. 15596026; Invitrogen; Thermo Fisher Scientific, Inc.) according to the manufacturer's instructions. The NanoDrop 2000 (Thermo Fisher Scientific, Inc.) was used to confirm the concentration and purity of abstracted

RNA. The PrimeScript™ RT reagent kit with gDNA Eraser (cat. no. RR047Q; Takara Biotechnology Co., Ltd.) was used to synthesize cDNA from 1 µg total RNA according to the manufacturer's instructions. qPCR was performed using SYBR Premix Ex Taq II (cat. no. RR820A) in StepOnePlus™ (Thermo Fisher Scientific, Inc.). The results were amplified using the following conditions: 40 Cycles at 95°C for 2 min, 95°C for 10 sec, 60°C for 40 sec. The relative mRNA expression of each group was normalized to β-actin and were calculated by $2^{-\Delta\Delta Cq}$ method (22). The ABCG2 primer sequences included sense primer (5'-TTCAGTACTTCAGCATTCCACGAT-3) and antisense primer (5'-ATTGTTTCCTGTTGCATTGAG TCC-3'). The β-actin primer sequences included sense primer (5'-GCACTCTTCCAGCCTTCCTTCC-3') and antisense primer (5'-TCACCTTCACCGTTCCAGTTTTT-3').

Cell apoptosis assay. The SSP, SSP-EV, SSP-ABCG2 and SSP-ABCG2-SH cells were collected in the 1x binding buffer (cat. no. 556454; BD Biosciences) at a concentration of $1x10^6$ cells/ml after 48 h serum-free culture at 37°C. In total, 5 µl APC Annexin V (cat. no. 561012; BD Biosciences) was used for staining for 15 min at RT in the dark. Next, 400 µl 1x binding buffer and 5 µl 7-AAD (cat. no. 559925; BD Biosciences) was added to each tube for the exclusion of non-viable cells. Cells were analyzes using flow cytometry with the FACSCantoII and FACSDiva software version 6.1.2 (BD Biosciences). The results were exported using FlowJo™ version 10 software (FlowJo LLC).

Transwell assay. A total of $1x10^6$ cells from the four lentiviral transfection groups in the logarithmic growth phase were placed in serum-free RPMI-1640 medium (Gibco; Thermo Fisher Scientific, Inc.) at 37°C overnight. The cells were resuspended in serum-free, IL-2-free RPMI-1640 medium and adjusted to a cell density of $1.5x10^5$ cells/ml. Cell suspension (200 µl) was added to the upper Transwell chamber, and 700 µl RPMI-1640 medium was added to the lower chamber. The migration of the underlying cells was observed under a light microscope (50x magnification; DMI400B; Leica Microsystems GmbH) after 24 h, cells in the lower compartment were collected and measured using the aforementioned CCK-8 method to evaluate migrated cells using a Multiskan FC microplate reader (absorbance: 450 nm, Thermo Fisher Scientific, Inc.).

Clone formation experiment. Four groups of cells were adjusted to a concentration of $1x10^4$ cells/ml. 90 µl of methylcellulose clone (Methylcellulose cell cloning kit; GENMED SCIENTIFICS INC, USA, GMS10003) was added to the suspension (clone:cell suspension, 9:1), and the cells were incubated in a 37°C water bath for 15 min. The cells were diluted (1:9) for testing, and the contents were mixed by shaking and transferred to a 24-well culture plate at 1 ml per well. Cells were incubated at 37°C for 5 days. Images were captured using a light microscope (50x magnification, DMI400B; Leica Microsystems GmbH).

In vivo transplantation to BALB/c nude mice. Animal experiments were approved by the Ethics Committee of Scientific Research/Medicine Clinical Trial of The First Affiliated

Hospital of Zhengzhou University (approval no. SS-2018-18; Zhengzhou, China). The guidelines of the Animal Care and Use Committee of Zhengzhou University were strictly implemented during the experiment. Twenty female 4-week-old BALB/c nude mice with a starting average weight of 21 g (Beijing Vital River Laboratory Animal Technology Co., Ltd.) were kept in the microisolator units in the standard barrier animal room under the automatic light control (light 12 h, dark 12 h), temperature 22˚C, relative humidity 60% and standard sterile laboratory diet (23) for 5 days before the experiment. Animal health was checked prior to before tumor grouping and implantation to ensure that the mice were disease-free. During the course of the experiment, animals were monitored once a day for laboratory condition, environment, dietary supply, mouse growth, activity and tumor burden. The mice were divided into four groups named SSP, SSP-EV, SSP-ABCG2 and SSP-ABCG2-SH at random and injected separately with SSP, SSP-EV, SSP-ABCG2 and SSP-ABCG2-SH cells with $1x10^6/100$ μl of serum-free RPMI-1640 medium in the same volume of Matrigel (BD Biosciences) into the right back side flank regions. The SSP-EV group was the negative control. When tumors were ~0.5 cm, gemcitabine (0.15 μg/ml, once every 5 days, intraperitoneally, Sigma-Aldrich; Merck KGaA) was used for drug intervention. As the tumor grew, the volume and weight were measured and recorded once a day with the following established formula: Tumor size = $(L1xL2^2)/2$, where L1 is the long axis and L2 is the short axis of the tumor. Thirty days posT cell injection, the largest tumor volume reached ~2,000 mm^3 and no mice died. The mice were humanely sacrificed by cervical dislocation, and tumor samples were harvested by standard forceps, scissors and surgical blades for further analysis.

Immunohistochemistry (IHC). Paraffin-embedded sections from xenograft tumors which were cut into 5-μm sections and were heated at 55˚C for deparaffinization. Remove the wax with xylene three times (20 min each time), and rehydrate the section with absolute ethanol for 10 min, 95% ethanol (diluted with distilled water) fir 5 min and 80% ethanol for 5 min. Rinse with distilled water 3 times. After antigen retrieval, the slides were incubated with the corresponding antibodies: Caspase 3 (1:50; cat. no. 19677-1-AP; ProteinTech Group, Inc.), Bax (1:400; cat. no. 5023; Cell Signaling Technology, Inc.), BCL2 (1:400; cat. no. 15071; Cell Signaling Technology, Inc.), c-Myc (1:400; cat. no. ab32072; Abcam), CD56 (1:2,000; cat. no. 14255-1-AP; ProteinTech Group, Inc.), CD3 (1:200; cat. no. 17617-1-AP; ProteinTech Group, Inc.) and Nucleolysin TIA-1 isoform p40 (TIA 1) (1:100; cat. no. 12133-2-AP; ProteinTech Group, Inc.) at 4˚C overnight. Following this, sections were incubated with Mouse and Rabbit-specific HRP/DAB (ABC) from the Mouse and Rabbit specific HRP/DAB (ABC) Detection IHC kit (cat. no. ab64264; Abcam). Epstein-Barr virus (EBV) RNA transcripts was performed using the RISH Epstein Barr encoded RNA probe kit (ISH-6022-Y, 170510; OriGene Technologies, Inc.). Images were captured using a light microscope (200x magnification, DMI400B; Leica Microsystems GmbH) and analyzed using ImageJ version 1.52a software (National Institutes of Health).

Terminal deoxynucleotidyl-transferase-mediated dUTP nick end labelling (TUNEL) assay. Paraffin-embedded sections were dewaxed, hydrated and rinsed (the same steps as IHC). The slices were incubated with TUNEL reagent from the One Step TUNEL Apoptosis Assay kit (cat. no. 1089; Beyotime Institute of Biotechnology) at 37˚C for 1 h in the darkness. DAPI (cat. no. D9542; Sigma-Aldrich; Merck KGaA) was used to dye the nuclei at RT for 30 min. Images were captured using a fluorescence microscope (200x magnification; DMI400B; Leica Microsystems GmbH) after dropwise adding the anti-fluorescence quenching mounting solution (cat. no. P0126-5; Beyotime Institute of Biotechnology). Ten fields of view were randomly selected for analysis, each containing 200 cells.

Statistical analysis. SPSS version 21.0 (IBM, Corp.) and GraphPad Prism version 7.0 were used to analyze the data. All data are reported as the mean ± SD (unless otherwise shown). Comparisons between and among groups were performed with unpaired two-tailed Student's t-test and one-way analysis of variance (ANOVA) followed by Bonferroni's correction for multiple comparisons. IC$_{50}$ values were calculated using the linear regression method. P<0.05 was considered to indicate a statistically significant difference.

Results

ABCG2 is upregulated in SSP cells. Increasing evidence indicates that SP cells are vital in cancer relapse (9,15). Our previous study showed SSP cells provided a new perspective to better understand the mechanisms of MDR in ENKL (15). However, the function of ABCG2 in SSP cells is unclear. To address this question, the expression of ABCG2 was measured. As expected, immunofluorescence (Fig. 1A and B) and western blotting (Fig. 1C) results showed that the expression of ABCG2 protein was significantly upregulated in SSP cells compared with SNK-6 cells (P<0.001). The specific properties of lymphocytic surface markers in SSP cells were analyzed. Flow cytometry showed SSP cells had NK-cell phenotype (CD56+, CD3-, CD8-, CD5-, CD16-, Granzyme B+ and Perforin+) compared with negative control (Fig. S1).

To further validate the effect of ABCG2 in on the proliferation of SSP cells, SSP cells were infected with a recombinant lentiviral vector, empty vector sequence of lentivirus for negative control (SSP-EV), lenti-ABCG2 for ABCG2 overexpression (SSP-ABCG2), lenti-sh negative control (SSP-sh-control) and three types of lenti-ABCG2 shRNAs for downregulation. Then, western blotting (Fig. 1D) and RT-qPCR (Fig. 1E) were used to screen out the most efficient cells (ABCG2-sh3, referred to as SSP-ABCG2-SH). In order to determine whether the cell proliferation caused by ABCG2 was due to its pro-proliferation effect or weakening of the antiproliferative effect of the drugs in SSP cells (due to the efflux activity of ABCG2), a CCK-8 assay was performed. The OD values among the five groups presented the same trend and were not significantly different (P>0.05; Fig. 1F), which showed that ABCG2 had no role in the proliferation of SSP cells without drug action. Collectively, these data suggested the expression of ABCG2 increased in SSP cells and ABCG2 had no effect on cell proliferation.

Altering the expression of ABCG2 can affect the drug resistance of SSP cells. The CCK-8 method was used to verify the MDR.
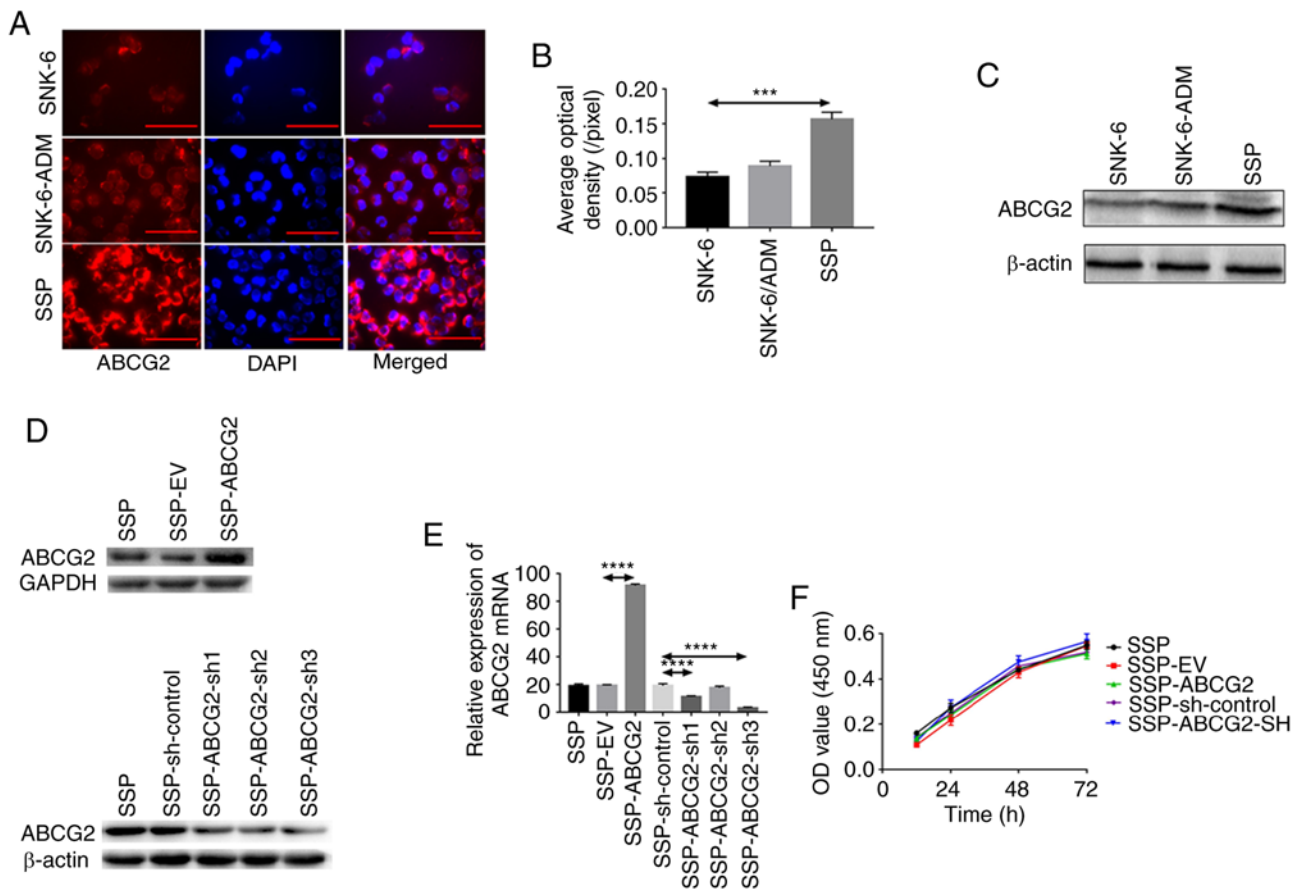
Figure 1. ABCG2 is upregulated in SSP cells. (A) The different expression levels of ABCG2 in SNK-6, SNK-6-ADM and SSP cells (400x magnification) were tested by immunofluorescence. Scale bar, 50 μm. (B) Corresponding statistical analysis of the images shown in panel A. (C) Western blotting was used to measure the expression levels of ABCG2 among the SNK-6, SNK-6-ADM and SSP cells and (D) detect the transduction efficiency in SSP-EV, SSP-ABCG2, SSP-ABCG2-sh1, SSP-ABCG2-sh2 and SSP-ABCG2-sh3 cells (D). (E) RNA extracted from the groups of cells was subjected to reverse transcription-quantitative PCR to obtain the relative expression of ABCG2. (F) The Cell Counting Kit-8 method was used to analyze whether ABCG2 had an effect on cell proliferation. Data are shown as the mean ± SD. n=3. ***P<0.001, ****P<0.0001. ABCG2, ATP-binding cassette subfamily G member 2; SSP, side population cells-SNK-6/ADM-SP; sh, short hairpin.

First, the impact of doxorubicin in the five groups was detected and it was observed that the inhibition rate of SSP-ABCG-SH was significantly higher compared with the SSP-EV and the SSP-sh-control group (P<0.05) under the same drug concentration (Fig. 2B). The SSP-EV and SSP-sh-control groups were both controls of the SSP-ABCG2 and SSP-ABCG2-SH groups, respectively, and these treatments both did not impact ABCG2 expression (Fig. 1D and E) or proliferation (Fig. 1F and 2B) regardless of drug intervention. SSP-EV was used for comparison in the following experiments because SSP-sh-control was only to ensure the specificity of ABCG2 shRNA (Fig. 1D, E) and to exclude potential interference of random sequence in the proliferation assay under drug (Fig. 2B) or not (Fig. 1F). Following treatment with cytarabine, cisplatin and gemcitabine, the inhibition rates of SSP-ABCG2 cells were lower compared with SSP-EV cells (P<0.05) with the same trend under doxorubicin (Fig. 2A, C and D). Furthermore, the IC$_{50}$ value of the cytarabine in SSP-ABCG2 cells killed 50% SSP-ABCG2 cells, but killed 90% SSP-ABCG2-SH cells (Fig. 2A). Therefore, SSP-ABCG2-SH cells had increased sensitivity to cytarabine compared with SSP-ABCG2 cells. In contrast, the inhibition rate difference did not exist in the four transfection groups treated with l-asparaginase (Fig. 2E).

The IC$_{50}$ values of the four transfection groups of cells were determined and the drug sensitivity was determined using the IC$_{50}$ values. As shown in Table I and Fig. 2F and G, when treated with doxorubicin, SSP-ABCG2 cells had a low level of sensitivity, with a significantly relatively higher IC$_{50}$ value of 107.293±1.77 compared with the SSP and SSP-EV cells (IC$_{50}$ values were 80.880±1.55 and 78.556±0.89), respectively, and SSP-ABCG2-SH cells were signifacantly highly sensitive, with an IC$_{50}$ value of 38.299±2.59 (P<0.01). The IC$_{50}$ values in cytarabine, cisplatin and gemcitabine presented the same trend as doxorubicin. In summary, SSP-ABCG2 cells were significantly less sensitive (higher IC$_{50}$ values) under doxorubicin, cytarabine, cisplatin and gemcitabine compared with SSP-EV cells, and SSP-ABCG2-SH cells were significantly sensitive. However, the IC$_{50}$ values of l-asparaginasum showed no change among the four transfection groups. In other words, these results indicated that l-asparaginasum had not been affected to MDR mechanisms in SSP cells compared with doxorubicin, cytarabine, cisplatin and gemcitabine.

Additionally, further tests were performed to determine whether the combination of two drugs can decrease drug resistance characteristics of cells. Notably, the results showed that the incorporation of two drugs still did not eliminate the
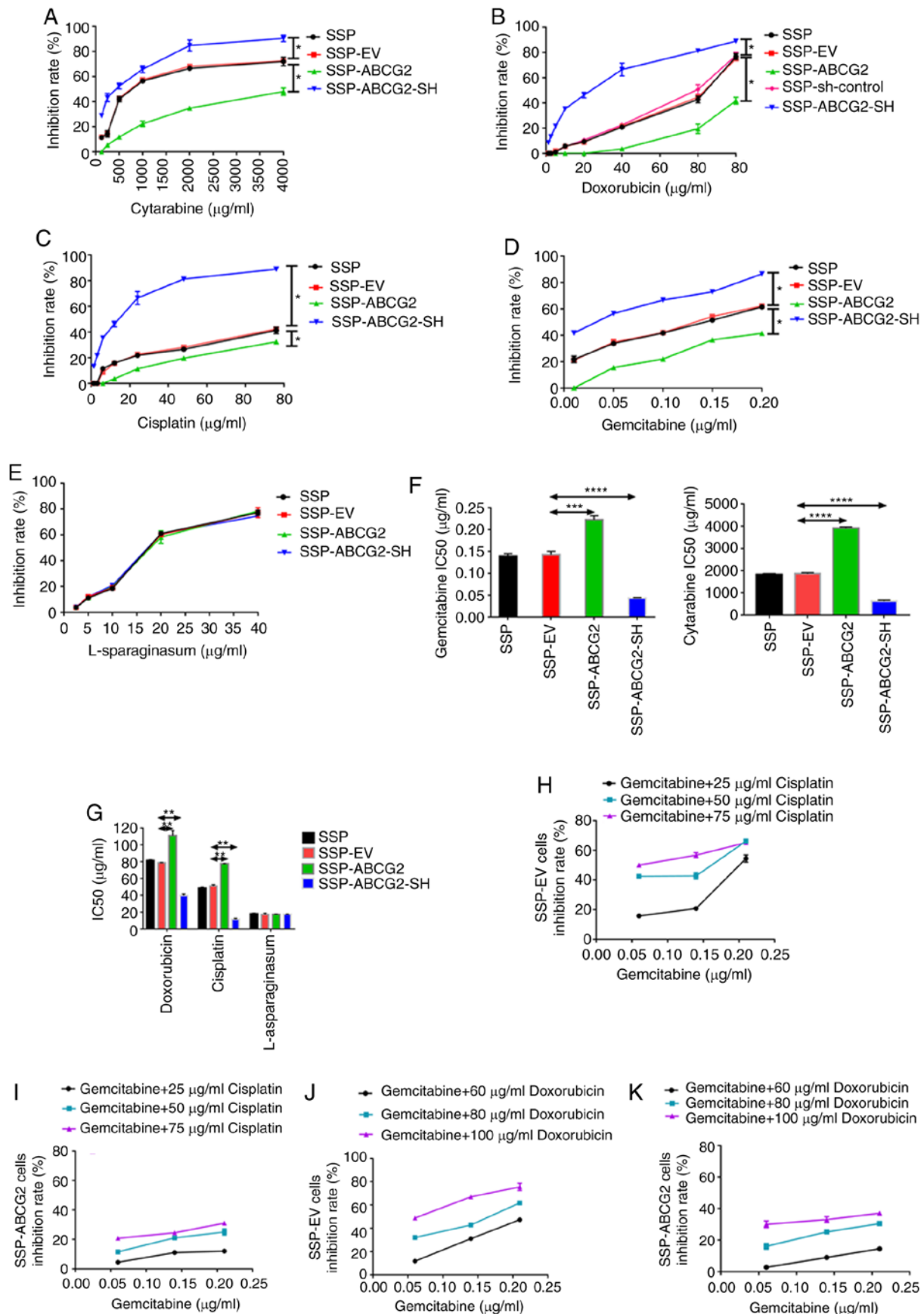
Figure 2. Altering the expression of ABCG2 can affect the drug resistance of SSP cells. SSP, SSP-EV, SSP-ABCG2, SSP-ABCG2-SH cells were separately treated with (A) cytarabine, (B) doxorubicin, (C) cisplatin, (D) gemcitabine and (E) l-asparaginasum. (A-E) show drug inhibition curves at various concentrations. The IC_{50} values among the four cell lines treated with cytarabine and gemcitabine (F) and doxorubicin, cisplatin and l-asparaginasum (G) are shown. Effects of the combined use of the (H and I) cisplatin-gemcitabine group and (J and K) doxorubicin-gemcitabine are presented in the SSP-EV cells (H and J) and SSP-ABCG2 cells (I and K). Data are shown as the mean ± SD, n=3. *P<0.05, **P<0.01, ***P<0.001, ****P<0.0001. ABCG2, ATP-binding cassette subfamily G member 2; SSP, side population cells-SNK-6/ADM-SP; sh, short hairpin.

Table I. IC$_{50}$ values of four different cell lines treated with five different chemotherapy drugs.

| | IC$_{50}$, μg/ml | | | |
Drug	SSP cells	SSP-EV cells	SSP-ABCG2 cells	SSP-ABCG2-SH cells
Doxorubicin	80.880±1.551	78.556±0.892	107.293±1.771[a]	38.299±2.591[a]
Cytarabine	1,800.598±4.832	1,788.376±8.241	3,900.468±5.772[c]	599.810±2.572[c]
Cisplatin	52.213±4.092	51.827±5.773	77.723±1.652[a]	10.983±3.669[a]
Gemcitabine	0.130±0.002	0.140±0.005	0.228±0.005[b]	0.043±0.001[c]
l-asparaginasum	18.950±1.081	18.770±1.338	18.000±0.988	17.880±0.771

Data are shown as the mean ± SD. [a]P<0.01, [b]P<0.001, [c]P<0.0001 vs. SSP-EV cells.
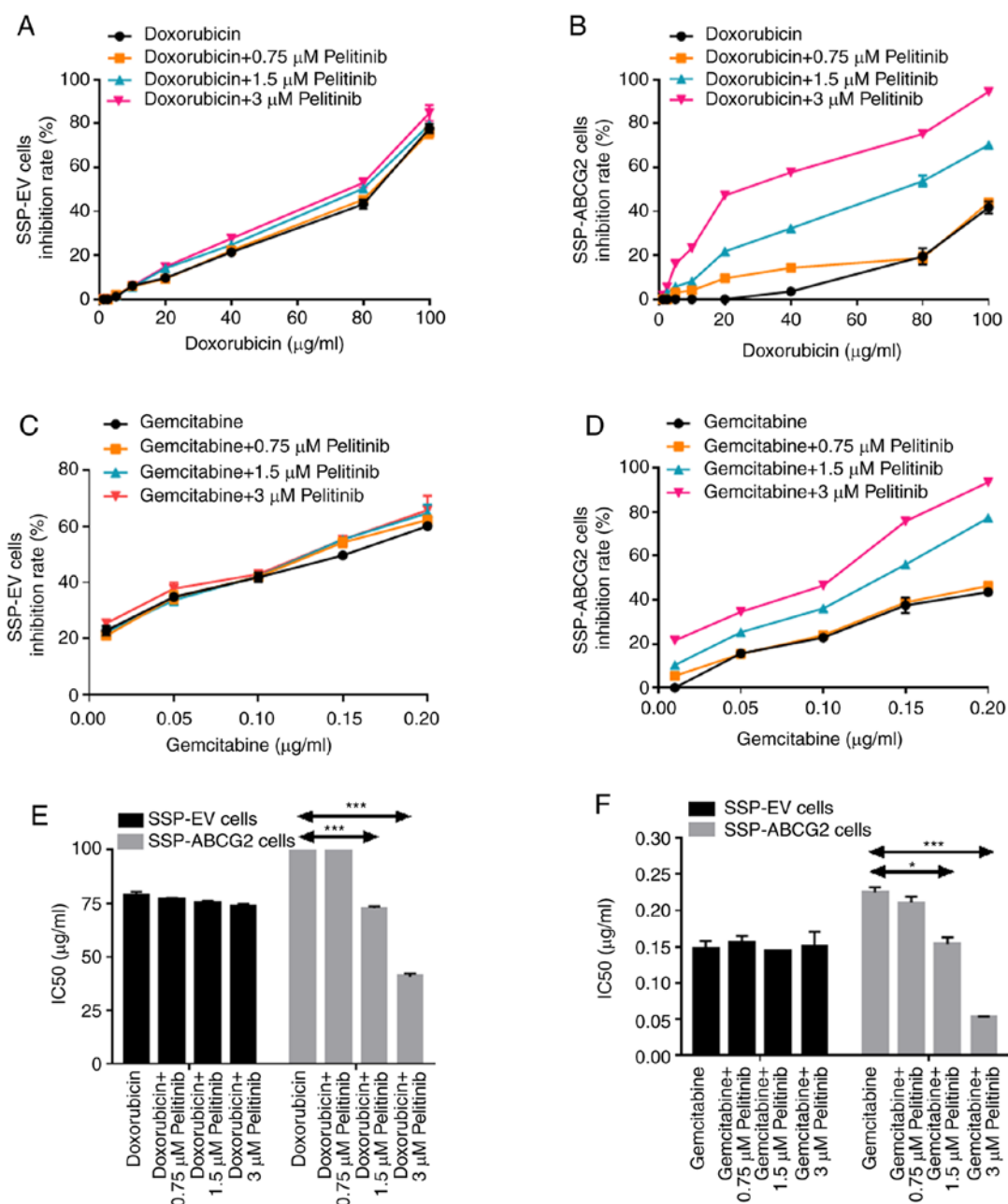

Figure 3. Pelitinib can overcome multidrug resistance induced by ABCG2. (A) The inhibition rate of doxorubicin in SSP-EV and (B) SSP-ABCG2 cells under the action of the inhibitor pelitinib. The inhibition rates of gemcitabine in (C) SSP-EV and (D) SSP-ABCG2 cells under pelitinib are shown. (E and F) IC$_{50}$ values of the two drugs under pelitinib. Data are shown as the mean ± SD, n=3. *P<0.05, ***P<0.001. ABCG2, ATP-binding cassette subfamily G member 2; SSP, side population cells-SNK-6/ADM-SP.

Table II. IC$_{50}$ values of SSP-EV and SSP-ABCG2 cell lines treated with different concentration of Pelitinib combined with Doxorubicin and Gemcitabine.

	IC$_{50}$, μg/ml	
Drug	SSP-EV cells	SSP-ABCG2 cells
Doxorubicin	78.819±1.640	106.786±1.660
Doxorubicin+0.75 μM Pelitinib	76.813±0.770	112.657±2.990
Doxorubicin+1.5 μM Pelitinib	75.307±0.890	72.828±0.770[a]
Doxorubicin+3 μM Pelitinib	73.563±1.220	40.895±1.390[a]
Gemcitabine	0.149±0.010	0.225±0.007
Gemcitabine+0.75 μM Pelitinib	0.156±0.009	0.221±0.008
Gemcitabine+1.5 μM Pelitinib	0.144±0.001	0.154±0.009[b]
Gemcitabine+3 μM Pelitinib	0.151±0.020	0.053±0.001[c]

Data are shown as the mean ± SD. [a]$P<0.001$ vs. Doxorubicin in SSP-ABCG2 cells, [b]$P<0.05$ vs. Gemcitabine in SSP-ABCG2 cells, [c]$P<0.001$ vs. Gemcitabine in SSP-ABCG2 cells.
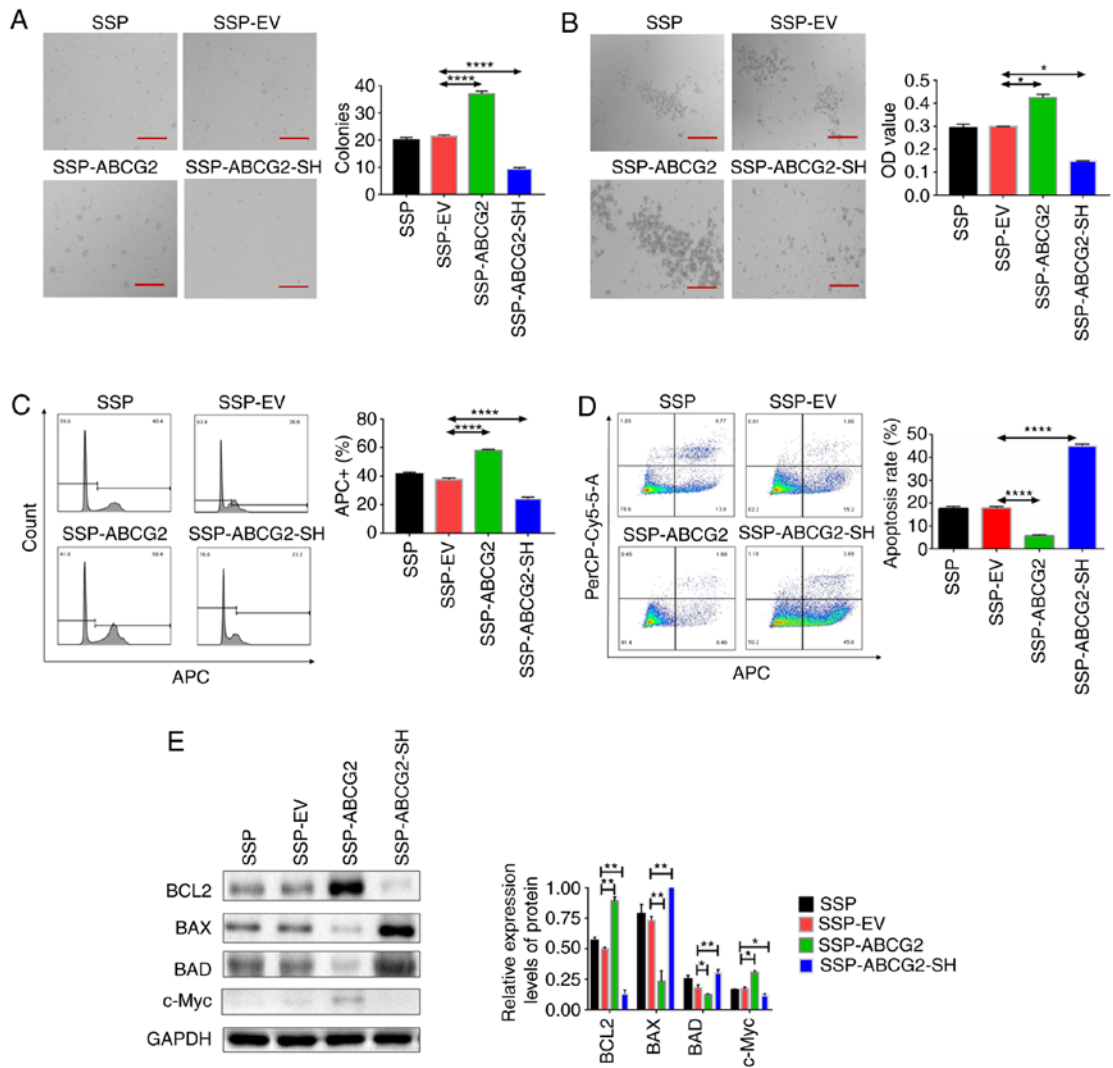

Figure 4. ABCG2 influences the proliferation and migration of gemcitabine-treated SSP cells. (A) Colony formation experiments (x50 magnification). Scale bar, 500 μm. (B) Transwell assays (x50 magnification). Scale bar, 50 μm. (C) EDU assays and (D) apoptosis analyses were performed using SSP cells with different ABCG2 expression levels after treatment with gemcitabine. (E) Western blotting was used to analyze different levels of apoptosis-related proteins (BCL2, Bax, BAD and c-Myc) in SSP, SSP-EV, SSP-ABCG2 and SSP-ABCG2-SH cells. Data are shown as the mean ± SD, n=3. *$P<0.05$, **$P<0.01$, ****$P<0.0001$. ABCG2, ATP-binding cassette subfamily G member 2; SSP, side population cells-SNK-6/ADM-SP; c-Myc, Myc proto-oncogene protein; APC, APC Annexin V.
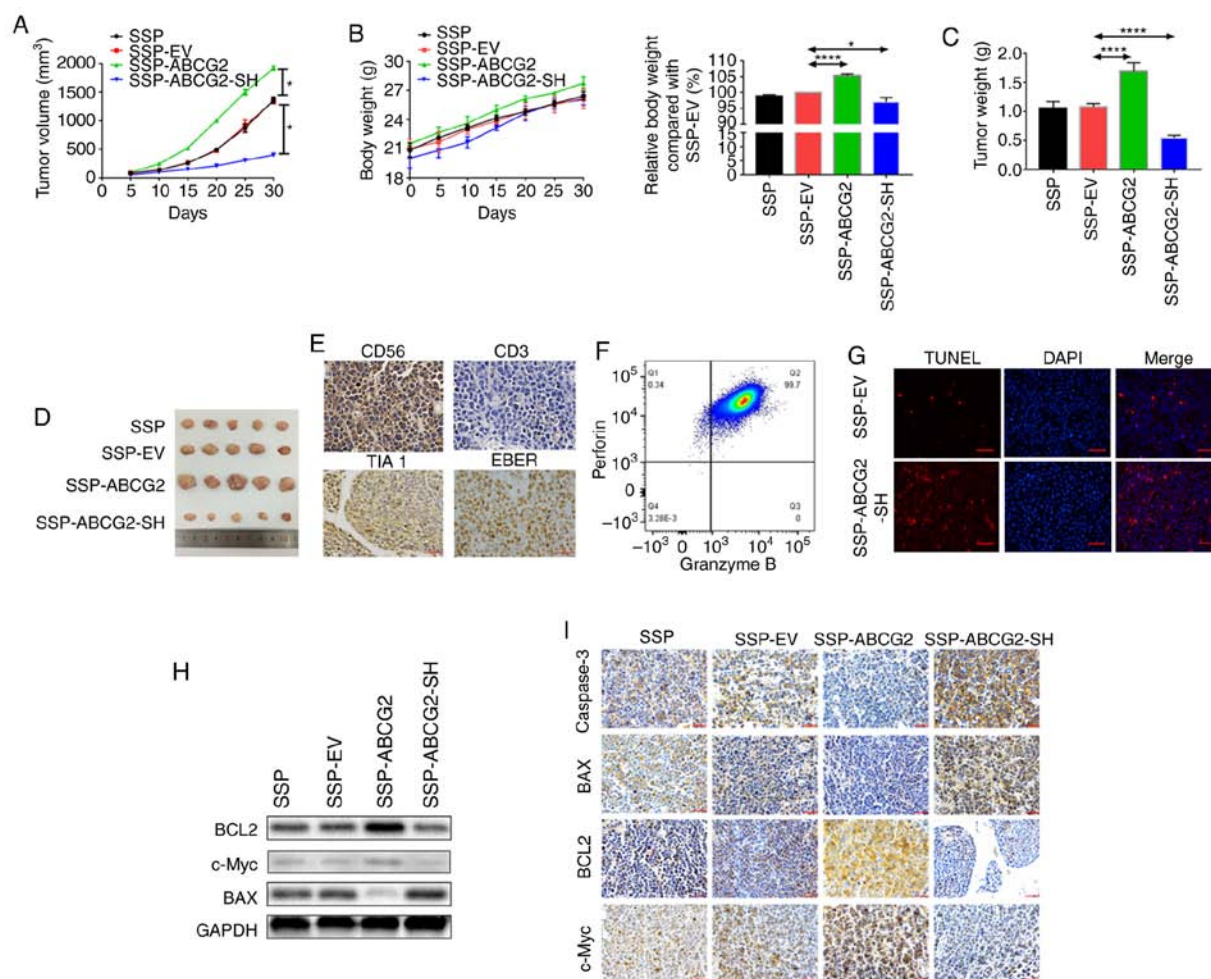
Figure 5. Altered ABCG2 expression significantly affects SSP tumor growth under the action of gemcitabine *in vivo*. (A) Mean average tumor volume, (B) mouse body weight and (C) tumor weight were calculated. (D) Xenograft tumors were measured every day until the mice were sacrificed. n=20. Lymphocytic surface molecular markers (CD56, CD3, TIA 1, EBER, Granzyme B and Perforin) were detected using (E) immunohistochemistry and (F) flow cytometry in the mouse model. Scale bar, 50 μm. (G) SSP-EV and SSP-ABCG2 cell-transplanted tumors were tested the number of apoptotic cells using terminal deoxynucleotidyl-transferase-mediated dUTP nick end labelling. Scale bar, 50 μm. (H) Western blotting was used to detect the expression levels of apoptotic proteins (Bax) and anti-apoptotic proteins (BCL2 and c-Myc) in each group of tumors. (I) Immunohistochemistry results showed BCL2, c-Myc, Bax and caspase 3 expression in each group of tumors. Scale bar, 50 μm. Data are shown as the mean ± SD, n=3. $^{*}P<0.05$, $^{****}P<0.0001$. ABCG2, ATP-binding cassette subfamily G member 2; SSP, side population cells-SNK-6/ADM-SP; EBER, EBV-encoded small RNA; TIA 1, nucleolysin TIA-1 isoform p40; c-Myc, Myc proto-oncogene protein.

multidrug resistance induced by ABCG2. The inhibition rates of SSP-ABCG2 cells (Fig. 2I and K) were far lower compared with the results of the SSP-EV cells (Fig. 2H and G), which showed no difference between treatment with cisplatin-gemcitabine group or doxorubicin-gemcitabine.

Pelitinib can overcome MDR induced by ABCG2. Once the potent effect of ABCG2 on MDR was observed, pelitinib, which is an inhibitor of ABCG2 (24-26), was selected to test the effects on SSP cells. Pelitinib, an irreversible epidermal growth factor receptor tyrosine kinase inhibitor, has been demonstrated to notably inhibit ABCG2 efflux activity by interfering with their ATPase activity (24) without the ABCG2 protein levels being impacted (25,26).

As shown in Fig. 3A-D, the inhibition rates of doxorubicin and gemcitabine were found to be enhanced by pelitinib in the SSP-ABCG2 cells in a concentration-dependent manner. In ABCG2-overexpression cells, the IC_{50} values of doxorubicin (Fig. 3E) and gemcitabine (Fig. 3F) were significantly declined in the presence of increasing pelitinib concentrations (Table II). The IC_{50} values could immune from 0.75 μM Pelitinib both in doxorubicin and gemcitabine (P>0.05). However, as shown in Table II when the concentration reached 1.5 μM, the IC_{50} values were significantly lower compared with non-pelitinib groups (P<0.05). The results suggested that pelitinib was resistant to the efflux mechanism of ABCG2, so that lower concentrations of the drugs could also kill the cells.

ABCG2 influences the proliferation and migration of gemcitabine-treated SSP cells. The results of the colony formation experiment (Fig. 4A) showed that the SSP-ABCG2 cells presented significantly higher density growth (P<0.0001) compared with SSP-EV cells, and the cytoplasm was bright, regular and round after treatment with gemcitabine. In contrast, SSP-ABCG2-SH cells showed significantly decreased cell proliferation (P<0.0001) compared with SSP-EV cells, and almost lost the ability to form colonies. Then, Transwell

assays were used to determine migration (Fig. 4B). The results indicated that ABCG2-knockdown decreased cell migration significantly compared with the SSP-EV cells (P<0.05).

EdU assays were conducted to investigate how ABCG2 regulated cell proliferation in gemcitabine-treated cells. It was demonstrated that SSP-ABCG2 cells significantly accounted for a larger proportion of cells in the log growth phase compared with SSP-EV cells (P<0.0001), and SSP-ABCG2-SH cells was significant far less compared with in SSP-EV cells (P<0.0001) (both Fig. 4C).

To examine whether ABCG2 has a functional role in regulating apoptosis with gemcitabine, flow cytometry was used. It was found that SSP-ABCG2-SH significantly induced apoptosis (P<0.001) and increasing the expression of ABCG2 decreased the rate of apoptosis significantly (P<0.001) (Fig. 4D). Then, the expression of apoptosis-associated genes was investigated in gemcitabine-treated cells. It was shown that pro-apoptotic proteins, such as Bax and Bad (27), were significantly upregulated (Fig. 4E) and anti-apoptotic proteins, such as BCL2 and C-myc (28), were significantly downregulated in ABCG2 overexpression cells compared with SSP-EV cells (P<0.05).

Altered ABCG2 expression significantly affects SSP tumor growth under the action of gemcitabine in vivo. In order to determine the role of ABCG2 on tumorigenicity, four groups of cells were injected into nude mice and tumor incidence was assessed. All mice developed tumors within half a month. When tumors were ~0.5 cm, they were treated with gemcitabine for 3 weeks. There was a significant inhibition of tumor volume (P<0.05; Fig. 5A) and weight (P<0.0001; Fig. 5C) in the SSP-ABCG2-SH cell group compared with the SSP-EV group. This result indicated thaT cells became more sensitive to gemcitabine when ABCG2 was downregulated. It was found that tumor volumes and weight were significantly higher in mice injected with SSP-ABCG2 cells (P<0.05; Fig. 5A, C and D) compared with the SSP-EV group, which is indicative of the ability of ABCG2 to induce MDR.

To identify ENKL in the mouse model, IHC was used to detect lymphocytic surface molecular markers and morphological features (CD56, CD3, TIA 1, EBER, Granzyme B and Perforin). IHC showed that the tissue cells were positive for CD56 and TIA 1, and negative for CD3 (Fig. 5E). EBV infection was notably demonstrated *in situ* hybridization for EBV RNA using the EBER probe (Fig. 5E). SSP cell suspensions cultured from tumor tissues after grinding were analyzed using flow cytometry. The positive expression of Granzyme B and Perforin provided evidence for the successful establishment of an ENKL mouse model (Fig. 5F). As a result, all morphology and molecular markers (Fig. 5E and F) demonstrated that mouse tumors were NK cell-derived lymphoma.

To examine the influence of ABCG2 on apoptosis-related genes, TUNEL (Fig. 5G), western blotting (Fig. 5H) and IHC (Fig. 5I) were performed. Red fluorescence with higher brightness and density of TUNEL in SSP-ABCG2-SH cells indicated the SSP-ABCG2-SH cells experienced higher levels of apoptosis in gemcitabine compared with SSP-EV cells (Fig. 5G). The results in Fig. 5H-I showed that overexpression of ABCG2 decreased the expression of pro-apoptotic proteins (caspase 3 and Bax) and increased anti-apoptotic proteins (BCL2 and c-Myc). As expected, caspase 3 and Bax levels

in the tumor were increased after ABCG2 downregulation. It was concluded that the efflux ability of ABCG2 could partly offset the ability of gemcitabine to cause apoptosis (Fig. 5G) and cause decrease of pro-apoptotic protein and increase of anti-apoptotic proteins under the gemcitabine (Fig. 5H-I).

Discussion

Of patients with ENKL, ~70% present with localized or early-stage disease, and despite the improvements of radiation therapy and chemotherapy, relapse occurs in ≤50% of patients with refractory and disseminated disease (4,5,29). The present study sought to exploit the upregulation of ABCG2 in SSP cells *in vivo* and *in vitro*, and utilize the combination of pelitinib with conventional anticancer drugs to specifically eradicate ENKL cancer cells. Most traditional chemotherapy drugs, such as doxorubicin, cytarabine, cisplatin and gemcitabine, could not overcome the drug resistance of SSP-ABCG2 cells, apart from l-asparaginasum, and even the combination of two drugs did not alleviate MDR.

SSP cells sorted from SNK-6 cells have been verified to exhibit the NK-cell phenotype (15). The xenograft tumors of SSP cells have also been detected the CD56+, TIA1+ and CD3- by IHC, Granzyme B+ and Perforin+ using flow cytometry, and EBER+ by *in situ* hybridization for EBV RNA. These lymphocytic surface molecular markers demonstrated the ENKL characteristics of these xenograft tumors.

Several studies have revealed that ABCG2 can be undoubtedly used as a biomarker to predict recurrence and poor outcomes in colon cancer (25,30-33). ABCG2-knockdown can also enhance the effect of cisplatin and attenuate the migration and invasion of squamous cell carcinoma (34). Therefore, targeting the ABC transporter superfamily and restoring sensitivity to chemotherapy has become an important goal for overcoming clinical drug resistance in cancer (35,36).

Several TKIs have been found to inhibit ABCG2. Afatinib leads to the methylation of the ABCG2 promoter and enhances the efficacy of conventional chemotherapeutic agents (37-39). One study revealed that ceritinib notably enhanced the efficacy of doxorubicin and paclitaxel in breast cancer (40). These studies were consistent with the results of the present study, which found that pelitinib can effectively increase tumor chemotherapy sensitivity by attenuating efflux activity in ENKL.

The association between ABCG2 and tumor characteristics has also been widely reported in various cancer types. ABCG2 was positively correlated with the abnormal activation of NF-κB in breast cancer (41) and matrix metalloproteinase 9 in glioma stem cells (42), but played a protective role against oxidative stress and inflammatory factors in colorectal cancer (43). It was of note that the relationship between the Wnt family and ABC family has been explored (44-49). Inhibition of Wnt/β-catenin signaling reversed multi-drug resistance of cholangiocarcinoma by reducing ABCB1 (48). Then researchers demonstrated that Wnt/β-catenin-ABCB1 signaling could be positively regulated by secreted frizzle-related protein 5 gene methylation in leukemia (44), retinoic acid receptor γ in colorectal cancer (45) and FZD1 in ovarian cancer (49) and negatively regulated by miR-506 in colorectal cancer (47). Knockdown of disheveled, a key mediator of Wnt/β-catenin, sensitized cisplatin-resistant

lung cancer cells through inhibiting ABCG2, ABCC, and ABCB1 (46). Therefore, it would be of value to investigate the relationship between ABCG2, Wnt/β-catenin and related regulatory genes in ENKL in the future.

However, the primary limitation of the present study is the lack of clinical tissue validation, although experiments conducted *in vitro* and *in vivo* and demonstrated the ENKL properties of cell line and xenograft tumors (CD3-, CD5-, CD8-, CD56+, CD16-, Granzyme B+, EBER+ and Perforin+). In the future, specimens from patients with ENKL should be used for pathological examination to detect ABCG2 expression and to guide treatment decisions according to pathological results. A study investigating the efficacy of drugs targeting ABCG2 would be preferable to validate the present results and this will be a focus of our future research.

In summary, the present study has provided additional insight to the MDR mechanisms of ENKL. It has been proposed that ABCG2 could be a promising biomarker for the identification of SP cells and a new therapeutic target for the eradication of SP cells due to its contribution to drug resistance, cell proliferation, apoptosis inhibition, distant metastasis and disease recurrence. Novel strategies targeting ABCG2 warrant further investigation. Such strategies could effectively circumvent drug resistance and eliminate the functions of SP cells to achieve improved cancer treatment.

Availability of data and materials

The data and materials in the current study are available from the corresponding author upon reasonable request.

Authors' contributions

SW and QC designed the study. SW, MD and ZY performed the experiments. SW analyzed experimental data and wrote the paper. QC and XZ revised the manuscript. All authors approved the final manuscript.

Ethics approval and consent to participate

Animal experiments were approved by the Ethics Committee of Scientific Research/Medicine Clinical Trial of The First Affiliated Hospital of Zhengzhou University (approval no. SS-2018-18; Zhengzhou, China).

Patient consent for publication

Not applicable.

Competing interests

The authors declare that they have no competing interests.

References

1. Jaccard A and Hermine O: A major turning point in NK/T-cell lymphoma? Blood 129: 2342-2343, 2017.
2. Tse E and Kwong YL: Nasal NK/T-cell lymphoma: RT, CT, or both. Blood 126: 1400-1401, 2015.
3. Haverkos BM, Pan Z, Gru AA, Freud AG, Rabinovitch R, Xu-Welliver M, Otto B, Barrionuevo C, Baiocchi RA, Rochford R and Porcu P: Extranodal NK/T cell lymphoma, nasal type (ENKTL-NT): An update on epidemiology, clinical presentation, and natural history in north American and european cases. Curr Hematol Malig Rep 11: 514-527, 2016.
4. Johnson WT and Mishra A: The EZ-riding NK/T-cell lymphoma. Blood 134: 1999-2000, 2019.
5. Somasundaram N, Lim JQ, Ong CK and Lim ST: Pathogenesis and biomarkers of natural killer T cell lymphoma (NKTL). J Hematol Oncol 12: 28, 2019.
6. Kucuk C, Jiang B, Hu X, Zhang W, Chan JKC, Xiao W, Lack N, Alkan C, Williams JC, Avery KN, *et al*: Activating mutations of STAT5B and STAT3 in lymphomas derived from γδ-T or NK cells. Nat Commun 6: 6025, 2015.
7. Chen YW, Guo T, Shen L, Wong KY, Tao Q, Choi WWL, Au-Yeung RKH, Chan YP, Wong MLY, Tang JCO, *et al*: Receptor-type tyrosine-protein phosphatase κ directly targets STAT3 activation for tumor suppression in nasal NK/T-cell lymphoma. Blood 125: 1589-1600, 2015.
8. Kwong YL, Chan TSY, Tan D, Kim SJ, Poon LM, Mow B, Khong PL, Loong F, Au-Yeung R, Iqbal J, *et al*: PD1 blockade with pembrolizumab is highly effective in relapsed or refractory NK/T-cell lymphoma failing l-asparaginase. Blood 129: 2437-2442, 2017.
9. Wang Y and Teng JS: Increased multi-drug resistance and reduced apoptosis in osteosarcoma side population cells are crucial factors for tumor recurrence. Exp Ther Med 12: 81-86, 2016.
10. Kim MC, D'Costa S, Suter S and Kim Y: Evaluation of a side population of canine lymphoma cells using Hoechst 33342 dye. J Vet Sci 14: 481-486, 2013.
11. Moti N, Malcolm T, Hamoudi R, Mian S, Garland G, Hook CE, Burke GAA, Wasik MA, Merkel O, Kenner L, *et al*: Anaplastic large cell lymphoma-propagating cells are detectable by side population analysis and possess an expression profile reflective of a primitive origin. Oncogene 34: 1843-1852, 2015.
12. Teshima K, Nara M, Watanabe A, Ito M, Ikeda S, Hatano Y, Oshima K, Seto M, Sawada K and Tagawa H: Dysregulation of BMI1 and microRNA-16 collaborate to enhance an anti-apoptotic potential in the side population of refractory mantle cell lymphoma. Oncogene 33: 2191-2203, 2014.
13. Yamazaki J, Mizukami T, Takizawa K, Kuramitsu M, Momose H, Masumi A, Ami Y, Hasegawa H, Hall WW, Tsujimoto H, *et al*: Identification of cancer stem cells in a tax-transgenic (Tax-Tg) mouse model of adult T-cell leukemia/lymphoma. Blood 114: 2709-2720, 2009.
14. Zabierowski SE and Herlyn M: Learning the ABCs of melanoma-initiating cells. Cancer Cell 13: 185-187, 2008.
15. Zhang X, Fu X, Dong M, Yang Z, Wu S, Ma M, Li Z, Wang X, Li L, Li X, *et al*: Conserved cell populations in doxorubicin-resistant human nasal natural killer/T cell lymphoma cell line: Super multidrug resistanT cells? Cancer Cell Int 18: 150, 2018.
16. Mo W and Zhang JT: Human ABCG2: Structure, function, and its role in multidrug resistance. Int J Biochem Mol Biol 3: 1-27, 2012.
17. Mao Q and Unadkat JD: Role of the breast cancer resistance protein (BCRP/ABCG2) in drug transport-an update. AAPS J 17: 65-82, 2015.
18. Noguchi K, Katayama K and Sugimoto Y: Human ABC transporter ABCG2/BCRP expression in chemoresistance: Basic and clinical perspectives for molecular cancer therapeutics. Pharmgenomics Pers Med 7: 53-64, 2014.
19. Nagata H, Konno A, Kimura N, Zhang Y, Kimura M, Demachi A, Sekine T, Yamamoto K and Shimizu N: Characterization of novel natural killer (NK)-cell and gammadelta T-cell lines established from primary lesions of nasal T/NK-cell lymphomas associated with the epstein-barr virus. Blood 97: 708-713, 2001.

20. Li Z, Zhang X, Xue W, Zhang Y, Li C, Song Y, Mei M, Lu L, Wang Y, Zhou Z, *et al*: Recurrent GNAQ mutation encoding T96S in natural killer/T cell lymphoma. Nat Commun 10: 4209, 2019.
21. Manska S, Octaviano R and Rossetto CC: 5-Ethynyl-2'-deoxycytidine and 5-ethynyl-2'-deoxyuridine are differentially incorporated in cells infected with HSV-1, HCMV, and KSHV viruses. J Biol Chem 295: 5871-5890, 2020.
22. Livak KJ and Schmittgen TD: Analysis of relative gene expression data using real-time quantitative PCR and the 2(-Delta Delta C(T)) method. Methods 25: 402-408, 2001.
23. Ghosh S and Mukherjee S: Testicular germ cell apoptosis and sperm defects in mice upon long-term high fat diet feeding. J Cell Physiol 233: 6896-6909, 2018.
24. To KKW, Poon DC, Wei Y, Wang F, Lin G and Fu L: Pelitinib (EKB-569) targets the up-regulation of ABCB1 and ABCG2 induced by hyperthermia to eradicate lung cancer. Br J Pharmacol 172: 4089-4106, 2015.
25. Ji N, Yang Y, Cai CY, Lei ZN, Wang JQ, Gupta P, Shukla S, Ambudkar SV, Kong D and Chen ZS: Selonsertib (GS-4997), an ASK1 inhibitor, antagonizes multidrug resistance in ABCB1- and ABCG2-overexpressing cancer cells. Cancer Lett 440-441: 82-93, 2019.
26. To KKW, Poon DC, Wei Y, Wang F, Lin G and Fu LW: Vatalanib sensitizes ABCB1 and ABCG2-overexpressing multidrug resistant colon cancer cells to chemotherapy under hypoxia. Biochem Pharmacol 97: 27-37, 2015.
27. Campbell GR, To RK and Spector SA: TREM-1 protects HIV-1-infected macrophages from apoptosis through maintenance of mitochondrial function. mBio 10: e02638-19, 2019.
28. Riedell PA and Smith SM: Double hit and double expressors in lymphoma: Definition and treatment. Cancer 124: 4622-4632, 2018.
29. de Mel S, Hue SSS, Jeyasekharan AD, Chng WJ and Ng SB: Molecular pathogenic pathways in extranodal NK/T cell lymphoma. J Hematol Oncol 12: 33, 2019.
30. Hu J, Li J, Yue X, Wang J, Liu J, Sun L and Kong D: Expression of the cancer stem cell markers ABCG2 and OCT-4 in right-sided colon cancer predicts recurrence and poor outcomes. Oncotarget 8: 28463-28470, 2017.
31. Farhana L, Nangia-Makker P, Arbit E, Shango K, Sarkar S, Mahmud H, Hadden T, Yu Y and Majumdar APN: Bile acid: A potential inducer of colon cancer stem cells. Stem Cell Res Ther 7: 181, 2016.
32. Di Desidero T, Orlandi P, Fioravanti A, Alì G, Cremolini C, Loupakis F, Gentile D, Banchi M, Cucchiara F, Antoniotti C, *et al*: Chemotherapeutic and antiangiogenic drugs beyond tumor progression in colon cancer: Evaluation of the effects of switched schedules and related pharmacodynamics. Biochem Pharmacol 164: 94-105, 2019.
33. Hsu HH, Chen MC, Baskaran R, Lin YM, Day CH, Lin YJ, Tu CC, Padma VV, Kuo WW and Huang CY: Oxaliplatin resistance in colorectal cancer cells is mediated via activation of ABCG2 to alleviate ER stress induced apoptosis. J Cell Physiol 233: 5458-5467, 2018.
34. Zhao L, Ren Y, Tang H, Wang W, He Q, Sun J, Zhou X and Wang A: Deregulation of the miR-222-ABCG2 regulatory module in tongue squamous cell carcinoma contributes to chemoresistance and enhanced migratory/invasive potential. Oncotarget 6: 44538-44550, 2015.
35. Peña-Solórzano D, Stark SA, König B, Sierra CA and Ochoa-Puentes C: ABCG2/BCRP: Specific and nonspecific modulators. Med Res Rev 37: 987-1050, 2017.
36. Sugimoto R, Watanabe H, Ikegami K, Enoki Y, Imafuku T, Sakaguchi Y, Murata M, Nishida K, Miyamura S, Ishima Y, *et al*: Down-regulation of ABCG2, a urate exporter, by parathyroid hormone enhances urate accumulation in secondary hyperparathyroidism. Kidney Int 91: 658-670, 2017.
37. Wang XK, He JH, Xu JH, Ye S, Wang F, Zhang H, Huang ZC, To KKW and Fu LW: Afatinib enhances the efficacy of conventional chemotherapeutic agents by eradicating cancer stem-like cells. Cancer Res 74: 4431-4445, 2014.
38. Wang XK, To KK, Huang LY, Xu JH, Yang K, Wang F, Huang ZC, Ye S and Fu LW: Afatinib circumvents multidrug resistance via dually inhibiting ATP binding cassette subfamily G member 2 in vitro and in vivo. Oncotarget 5: 11971-11985, 2014.
39. van Hoppe S, Sparidans RW, Wagenaar E, Beijnen JH and Schinkel AH: Breast cancer resistance protein (BCRP/ABCG2) and P-glycoprotein (P-gp/ABCB1) transport afatinib and restrict its oral availability and brain accumulation. Pharmacol Res 120: 43-50, 2017.
40. Hu J, Zhang X, Wang F, Wang X, Yang K, Xu M, To KKW, Li Q and Fu L: Effect of ceritinib (LDK378) on enhancement of chemotherapeutic agents in ABCB1 and ABCG2 overexpressing cells in vitro and in vivo. Oncotarget 6: 44643-44659, 2015.
41. Zhang W, Ding W, Chen Y, Feng M, Ouyang Y, Yu Y and He Z: Up-regulation of breast cancer resistance protein plays a role in HER2-mediated chemoresistance through PI3K/Akt and nuclear factor-kappa B signaling pathways in MCF7 breast cancer cells. Acta Biochim Biophys Sin (Shanghai) 43: 647-653, 2011.
42. Gong W, Wang Z, Wan Y, Shi L and Zhou Y: Downregulation of ABCG2 protein inhibits migration and invasion in U251 glioma stem cells. Neuroreport 25: 625-632, 2014.
43. Nie S, Huang Y, Shi M, Qian X, Li H, Peng C, Kong B, Zou X and Shen S: Protective role of ABCG2 against oxidative stress in colorectal cancer and its potential underlying mechanism. Oncology Rep 40: 2137-2146, 2018.
44. Wang H, Wang X, Hu R, Yang W, Liao A, Zhao C, Zhang J and Liu Z: Methylation of SFRP5 is related to multidrug resistance in leukemia cells. Cancer Gene Ther 21: 83-89, 2014.
45. Huang GL, Song W, Zhou P, Fu QR, Lin C, Chen QX and Shen DY: Oncogenic retinoic acid receptor γ knockdown reverses multi-drug resistance of human colorectal cancer via Wnt/β-catenin pathway. Cell Cycle 16: 685-692, 2017.
46. Luo K, Gu X, Liu J, Zeng G, Peng L, Huang H, Jiang M, Yang P, Li M, Yang Y, *et al*: Inhibition of disheveled-2 resensitizes cisplatin-resistant lung cancer cells through down-regulating Wnt/β -catenin signaling. Exp Cell Res 347: 105-113, 2016.
47. Zhou H, Lin C, Zhang Y, Zhang X, Zhang C, Zhang P, Xie X and Ren Z: miR-506 enhances the sensitivity of human colorectal cancer cells to oxaliplatin by suppressing MDR1/P-gp expression. Cell Prolif 50: e12341, 2017.
48. Shen DY, Zhang W, Zeng X and Liu CQ: Inhibition of Wnt/β -catenin signaling downregulates P-glycoprotein and reverses multi-drug resistance of cholangiocarcinoma. Cancer Sci 104: 1303-1308, 2013.
49. Zhang H, Jing X, Wu X, Hu J, Zhang X, Wang X, Su P, Li W and Zhou G: Suppression of multidrug resistance by rosiglitazone treatment in human ovarian cancer cells through downregulation of FZD1 and MDR1 genes. Anticancer Drugs 26: 706-715, 2015.